CoA Memo M and P No. 11

November, 1963

THE COLLEGE OF AERONAUTICS

DEPARTMENT OF PRODUCTION AND INDUSTRIAL ADMINISTRATION

Introducing strain-rate dependent work material properties into the analysis of orthogonal cutting[1]

- by -

P.L.B. Oxley[2]

SUMMARY

An analysis is presented in which cutting speed, depth of cut and certain strain-rate dependent work material properties are taken into account. Good agreement between theory and experiment is shown over a wide range of cutting conditions.

---

1 Paper prepared for presentation to members of CIRP.

2 The College of Aeronautics, Cranfield.

Contents

1. Introduction

In orthogonal cutting the cutting edge of the tool is parallel to the work surface and perpendicular to the cutting direction, and if the depth of cut (t in Fig. 1) is small compared to its width then the removed metal chip is formed under approximately plane strain conditions. Following the well known Ernst[1] definition the chip can be discontinuous, i.e. in which fracture occurs and the chip is made up of segments; continuous, i.e. formed by plastic deformation; or continuous but with a built-up edge which builds-up and breaks-down in a cyclic fashion. Only when cutting a continuous chip without a built-up edge does the process approximate to a steady state process and because of this it is usual to limit analytical work to cutting with this type of chip.

By taking ciné films through a microscope of the side of a cut during the actual cutting process it has been found that the continuous type chip is formed in a plastic zone which is of the shape shown in Fig. 1. (cutting speed $\frac{1}{2}$ in/min) and Fig. 2 (cutting speed 50 ft/min). If the viewed side of the work is polished and etched prior to cutting and filming then on projecting the ciné films the paths of flow of individual grains in the metal can be followed and recorded. Streamlines of flow obtained in this way (Figs. 1 and 2) can be seen to follow smooth, well defined curves from the work into the chip. The streamlines in the chip follow circular arcs which can be drawn from a common centre and the chip only contacts the tool for a certain length before curling away.

In analysing this process the known information would include the depth of cut t (Fig. 1), the rake angle α and the cutting speed. In addition we can suppose that the relevant mechanical and physical properties of the work and tool materials and the physical condition along the tool-chip interface are known. From this information our analysis should enable us to calculate the size and shape of the plastic zone; the thickness and curvature of the chip; the length of tool-chip contact; and the stresses, strains, strain rates and temperatures in the plastic zone and in the tool and chip material adjacent to the tool-chip interface. With an analysis of this kind, a much better understanding could be obtained of such practical problems as tool wear; the mechanical and physical properties of the machined surface including residual stresses; the transition from a continuous to a discontinuous chip; the formation of a built-up edge; and the cutting forces required.

The majority of investigators have simplified the problem by assuming that the chip is formed by simple shear across a single straight shear plane (AB in Fig. 3), with the chip straight and not curled. It is implicit in all solutions based on this shear plane model of chip formation that the state of stress along the shear plane is constant. The frictional condition along the tool-chip interface is represented by a mean angle of friction. Equations are obtained for the shear angle (ϕ in Fig. 3) in terms of the mean angle of friction λ and the tool rake angle α.

The best known of these equations is that due to Merchant[2] who assumed

that the shear angle would be such as to make the expenditure of work in cutting a minimum. This gave:

$$\phi = \frac{\pi}{4} + \frac{\alpha}{2} - \frac{\lambda}{2} \qquad (1)$$

Another well known equation was derived by Lee and Shaffer[3], namely:

$$\phi = \frac{\pi}{4} + \alpha - \lambda \qquad (2)$$

For a given value of $\lambda - \alpha$ both of these equations give a single value for ϕ. Figure 4 shows experimental values of ϕ for a wide range of cutting conditions and materials and it is clear from these results that no such simple linear relation exists.

There have been a number of attempts to modify both equations (1) and (2) in order to obtain better agreement with experiment. The most notable of these was by Merchant[2] himself. In deriving equation (1) he had assumed that the shear strength along the shear plane was independent of the normal stress on this plane. By taking account of the possible dependence of shear strength on normal stress Merchant obtained the equation

$$2\phi = C + \alpha - \lambda \qquad (3)$$

where C is a constant for a given material and represents the dependence of the shear strength on the normal stress. By giving C different values better agreement can be obtained between theory and experiment. Unfortunately the variation of shear strength with normal stress required to satisfy cutting data is too large.

More recently Kobayashi and Thomsen[4] have introduced the concept of effectiveness which is essentially a measure of the departure from the minimum energy solution of Merchant, i.e. equation (1). An effectiveness of unity corresponds to equation (1) and smaller values of effectiveness give a lower value of ϕ for a given value of $\lambda - \alpha$ than equation (1). By choosing suitable values of effectiveness it is possible to satisfy any experimental value of ϕ. Although useful in collating experimental data e.g. it appears that effectiveness is constant for a given material and cutting speed, the value of the analysis is limited by the lack of any obvious fundamental relationship between effectiveness and work material properties or cutting speed.

It can be seen that even the simplified shear angle problem has not been satisfactorily solved. Indeed it now seems that the shear plane model of chip formation is too far removed from actual chip formation to allow a successful solution. Experiments show that cutting process is highly dependent on the cutting speed and yet, except for associated variations in friction angle λ, speed is not taken into account in shear angle solutions. If instead of basing the analysis on the shear plane

model of chip formation a finite shear zone is considered then cutting speed can be introduced into the analysis in terms of the strain-rate in the shear zone. It is then possible to take account of those material properties which are strain-rate dependent. This paper presents such an analysis.

2. Theory

Let us assume:

(1) That the work material is an isotropic, plastic-rigid material in which the flow stress can vary with strain-rate, strain-hardening, etc.;

(2) that the removed metal chip is continuous without built-up edge and is formed under plane strain, orthogonal cutting conditions;

(3) that the chip is formed in a finite shear zone which has straight parallel sides as shown in Fig. 5, with AB, CD and EF representing shear lines, i.e. directions of maximum shear stress and maximum shear strain-rate (it is implicit in this assumption that the chip is straight and not curled, and that the shear strain and hence the shear stress is constant along each of the shear lines AB, CD and EF);

(4) that the cutting tool is perfectly sharp and that the resultant cutting face is transmitted by the rake face of the tool.

Following assumption (4) the shear line AB (Fig. 5) will transmit the resultant cutting force and it is convenient to base our analysis on the stress distribution along AB. For equilibrium the resultant across AB must be equal in magnitude and must act along the same line as the resultant transmitted by the tool along the tool-chip interface. Our method of analysis will be to analyse the stresses along AB in terms of the cutting conditions, material properties and ϕ (the angle made by AB with the direction of cutting) and then to select ϕ so that the stress distributions along AB and the tool-chip interface are consistent. From a geometrical point of view AB can be looked upon as the shear plane and ϕ as the shear angle, that is, from Fig. 5.

$$\tan \phi = \frac{t/T \cos \alpha}{1 - t/T \sin \alpha} \qquad (4)$$

where t is the depth of cut, T is the chip thickness and α is the tool rake angle, and this equation is the same as that derived by Merchant for the shear plane.

The shear stress on AB is the shear flow stress k and the normal stress is the hydrostatic stress p. In all shear plane solutions p is assumed constant along AB. Consider the equilibrium of the small element of the

shear zone shown in Fig. 6. As the material passes through the shear zone its shear flow stress will change, as a result of strain-hardening temperature etc. Therefore, let the shear flow stress along CD (i.e. initial shear flow stress at zero plastic strain) be $k - \frac{\Delta k}{2}$, and let the shear flow stress along EF be $k + \frac{\Delta k}{2}$. The total change in shear flow stress is then Δk. Resolving forces parallel to AB gives

$$\Delta p = \frac{\Delta k}{\Delta s_1} \Delta s_2 \tag{5}$$

where Δp is the change in hydrostatic stress across the element, Δs_1 is the width of the shear zone and Δs_2 is measured along AB. According to this equation the hydrostatic stress along AB must vary for a material whose shear flow stress changes during cutting. Applying this equation between A and B and noting that $\frac{\Delta k}{\Delta s_1}$ is constant along AB we obtain

$$p_A - p_B = \frac{\Delta k}{\Delta s_1} \cdot \frac{t}{\sin \phi} \tag{6}$$

or

$$p_B = p_A - \frac{\Delta k}{\Delta s_1} \frac{t}{\sin \phi}$$

where p_A is the hydrostatic stress at A (i.e. normal stress on AB at A) and p_B is the hydrostatic stress at B (i.e. normal stress on AB at B). For a constant value of $\frac{\Delta k}{\Delta s_1}$ along AB the variation in hydrostatic stress along AB will be linear and the total normal force per unit width acting on AB (see Fig. 14) will be

$$F_N = \frac{p_A + p_B}{2} \frac{t}{\sin \phi} \tag{7}$$

The corresponding shear force on AB will be

$$F_s = k \frac{t}{\sin \phi} \tag{8}$$

If then the angle made by the resultant cutting force with AB is θ (Fig. 5) we have

$$\tan \theta = \frac{F_N}{F_s} = \frac{p_A + p_B}{2k} \tag{9}$$

In a detailed analysis[5] of the plastic zone it was found that the hydrostatic stress in the region of A could be calculated most reliably from the free surface condition in the work material between C and A (Fig. 5),

the free surface becoming cracked and therefore irregular between A and E. Consider a shear line $A_1A_2A_3B_1$ adjacent to AB as shown in Fig. 7, with A_3B_1 parallel to AB. In order to satisfy equilibrium $A_1A_2A_3B_1$ as a line of maximum shear stress must meet the free surface at 45° and the hydrostatic stress in the triangular zone $A\,A_1A_2$ must be equal to the shear flow stress in this region. From physical considerations this hydrostatic stress will be compressive. p_A can now be found by considering the equilibrium of the element $A\,A_2A_3$. Taking moments about A gives

$$p_A = k\left\{1 + 2(\pi/4 - \phi)\right\} \tag{10}$$

If p_A is known, then equation (6) can be used to calculate p_B. In this equation Δk is the change of shear flow stress occuring in the shear zone. If we idealize the shear flow stress - shear strain curve of the work material as shown in Fig. 8, then

$$\Delta k = m\,\gamma \tag{11}$$

where m is the slope of the plastic stress-strain curve at the corresponding mean shear strain rate in the shear zone and γ is the shear strain along EF (Fig. 5). Before this equation can be used it is necessary to know the mean shear strain rate in the shear zone $\dot{\gamma}_{mean}$ and also the shear strain γ.

The maximum shear strain rate $\dot{\gamma}_{max}$ (i.e. the shear strain rate in the direction of the shear lines AB, CD and EF) can be expressed in the usual way in terms of the velocities of flow, that is,

$$\dot{\gamma}_{MAX} = \sqrt{\left(\frac{\partial u}{\partial y} + \frac{\partial v}{\partial x}\right)^2 + 4\left(\frac{\partial u}{\partial x}\right)^2} \tag{12}$$

where u and v are the velocities in the x and y directions respectively (see Fig. 9). To calculate the mean (maximum) shear strain rate in the shear zone we can consider a single finite step and measure Δu, Δv, Δx and Δy as shown in Fig. 9, that is,

$$\begin{aligned} \Delta u &= \frac{-U\cos\alpha\cos\phi}{\cos(\phi - \alpha)} \\ \Delta v &= \frac{U\cos\alpha\sin\phi}{\cos(\phi - \alpha)} \\ \Delta x &= \Delta s_1/\sin\phi \\ \Delta y &= \Delta s_1/\cos\phi \end{aligned} \tag{13}$$

where Δs_1 is the width of the shear zone and U is the work velocity. Substituting these values in equation (12) gives

$$\dot{\gamma}_{mean} = \frac{U \cos \alpha}{\Delta s_1 \cos(\phi - \alpha)} \tag{14}$$

or if U is in f.p.m. and Δs_1 is in in.

$$\dot{\gamma}_{mean} = \frac{0.2\ U \cos \alpha}{\Delta s_1 \cos(\phi - \alpha)} \text{ per sec.} \tag{15}$$

The shear strain along EF can be found by multiplying the mean shear strain rate by the time a particle takes to cross the shear zone. This gives

$$\gamma = \frac{\cos \alpha}{\sin \phi \cos(\phi - \alpha)} \tag{16}$$

It is now possible to calculate the stress distribution along AB and hence θ (Fig. 5) for any value of ϕ provided that certain work material properties (e.g. slope m) and the size of the shear zone are known.

The angle θ can also be expressed in terms of the frictional condition along the tool chip-interface and if for the moment we follow the usual practice and represent this frictional condition by a mean angle of friction λ, then

$$\theta = \phi + \lambda - \alpha \tag{17}$$

For given values of λ and α, ϕ is selected to give the same value of θ in equations (9) and (17) that is, the stress distributions along the shear line AB and the tool-chip interface are made consistent for the direction of the resultant cutting force. The condition that the position of the resultant should be consistent for both stress distributions is used later in the paper when considering the actual stress distribution along the tool-chip interface.

3. Shear angle calculations

Before the theory developed in the last section can be used to calculate the shear angle ϕ some assumption must be made about the size of the shear zone. From the experimental work of Kececioglu[6] and Nakayama[7] at relatively high cutting speeds and of Enaharo[8], and Palmer and Oxley[5] at low cutting speeds it appears that the ratio of the length to the mean width of the shear zone $\left(\frac{t}{\Delta s_1 \sin \phi}\right)$ lies between 6 and 12 for a range of cutting conditions

and work materials. Although this work is far from conclusive it would suggest that as a first step this ratio can be assumed constant. For the purpose of our calculations we will assume that

$$\frac{t}{\Delta s_1 \sin \phi} = 10 \qquad (18)$$

For the work material the relation between the slope m and shear strain rate, and between the initial shear flow stress and shear strain rate must be known. Although independent measurements of the variation of initial shear flow stress with strain rate have been made the author is not aware of similar measurements of the slope m over the required range of shear strain. In view of this curves of m and initial shear flow stress derived by the author[9] from cutting data[6] will be used in the calculations. These are given in Figs. 10 and 11 and it can be seen that for the steel considered (SAE 1015, 118 Bhn) the slope m decreases with increase in shear strain rate while the initial shear flow stress increases. For steel, these are expected trends.

In making the calculations the most convenient method is to assume a particular value of ϕ, for given conditions of rake angle, depth of cut and cutting speed, and then to work through the equations to find the corresponding value of friction angle λ. Graphs of ϕ against $\lambda - \alpha$ can then be plotted in the usual way.

Let us now consider a specimen calculation using the following cutting conditions:

rake angle α = 10°
depth of cut t = 0.008 in.
cutting speed U = 100 f.p.m.

Assume $\phi = 25°$

from Eqn. (18) $\Delta s_1 = 0.0019$ in.

from Eqn. (15) $\dot{\gamma} = 10700$ per sec.

referring to Figs. 10 and 11

$m = 1.8$ tons/in^2 and the initial shear flow stress

$(k - \frac{\Delta k}{2}) = 29.0$ tons/in^2

from Eqn. (16) $\gamma = 2.41$

from Eqn. (11) $\Delta k = 4.35$ tons/in^2

the shear flow stress, k, on AB is given by

$$k = \left(k - \frac{\Delta k}{2}\right) + \frac{\Delta k}{2}$$

$$= 31.2 \text{ tons/in}^2$$

from Eqn. (10) $p_{A/k} = 1.7$

from Eqn. (6) $(p_A - p_B)/k = 1.4$

hence $p_{B/k} = .3$

from Eqn. (9) $\theta = 45°$

from Eqn. (17) $\lambda - \alpha = 20°$

For $\alpha = 10°$, $\lambda = 30°$, we can now say that the analysis gives $\phi = 25°$. Using this method values of ϕ have been calculated, for a range of cutting conditions and are given in Figs. 12 and 13. Experimental values of ϕ calculated from equation (4) are also given.

It can be seen that the present theory is dependent on cutting speed (Fig. 12) and predicts that for given values of friction angle λ and rake angle α a decrease in cutting speed will lead to a decrease in ϕ. The experimental results support this. The influence of varying the depth of cut is shown in Fig. 13 and again the predicted trend is in agreement with epxerimental results.

4. Cutting force calculations

The resultant cutting force can be resolved into its various components as shown in Fig. 14 (see ref. 2). The forces which are usually measured in cutting tests are the force in the direction of cutting F_c and the force normal to this F_T. The force F_c is the force against which work is done and is therefore important in calculating the cutting horsepower.

From Fig. 14 it is easily shown that

$$F_c = \frac{t\, w\, k \cos(\lambda - \alpha)}{\sin\phi \cos(\phi + \lambda - \alpha)} \qquad (19)$$

and

$$F_T = \frac{t\, w\, k \sin(\lambda - \alpha)}{\sin\phi \cos(\phi + \lambda - \alpha)} \qquad (20)$$

where w is the width of cut.

Let us now use the theory to calculate F_c and F_T for the following cutting conditions:

rake angle α = 33°
depth of cut t = 0.004 in.
width of cut w = .169 in.
cutting speed U = 746 f.p.m.
work material SAE 1015 (118 BHN)

For these conditions the experimental value of ϕ was found to be 25.5°. Taking this value (we could equally well start with the experimental value of λ) we find that

$$\dot{\gamma} = 176000 \text{ per sec} \qquad \text{(from Eqn. 15)}$$

$$\gamma = 1.96 \qquad \text{(from Eqn. 16)}$$

$$m = .75 \text{ tons/in}^2 \qquad \text{(from Fig. 10)}$$

$$k - \frac{\Delta k}{2} = 34 \text{ tons/in}^2 \qquad \text{(from Fig. 11)}$$

$$\Delta k = 1.47 \text{ tons/in}^2 \qquad \text{(from Eqn. 11)}$$

$$\therefore \quad k = 34.7 \text{ tons/in}^2$$

$$p_{A/k} = 1.68 \qquad \text{(from Eqn. 10)}$$

$$(p_A - p_B)/k = .42 \qquad \text{(from Eqn. 6)}$$

$$\therefore \quad p_{B/k} = 1.26$$

$$\theta = 53.8° \qquad \text{(from Eqn. 9)}$$

$$\lambda - \alpha = 28.3° \qquad \text{(from Eqn. 17)}$$

$$\therefore \quad \lambda = 61.3°$$

Substituting in equations (19) and (20) gives

$$F_c = 178 \text{ lb.}$$

$$F_T = 96 \text{ lb.}$$

The corresponding experimentally measured values are

$$\lambda = 57.5°$$

$$F_c = 182 \text{ lb.}$$

$$F_T = 84 \text{ lb.}$$

It is of interest to note that if the depth of cut t is decreased with all other cutting conditions kept constant, then, according to the theory (equation (15)), the shear strain rate $\dot{\gamma}$ is increased and as a result of this the initial shear flow stress is increased (Fig. 11). This is a possible explanation for the increase in specific cutting pressure (F_c/area of cut) which occurs when t is decreased - the so called 'size effect' in metal cutting.

5. Tool-chip interface stresses

The mean normal stress on the tool face σ is given by

$$\sigma = \frac{N}{h\ w} \tag{21}$$

where h is the length of tool-chip contact, w is the width of cut and N (Fig. 14) is the force normal to the tool face. Substituting for N gives

$$\sigma = \frac{t\ k \cos \lambda}{h \sin \phi \cos (\phi + \lambda - \alpha)} \tag{22}$$

The mean shear stress on the tool face τ is given by

$$\tau = \frac{t\ k \sin \lambda}{h \sin \phi \cos (\phi + \lambda - \alpha)} \tag{23}$$

Clearly, before σ and τ can be calculated it is necessary to know h.

Experiments[10] have been made in which h was measured directly by examining the wear on the tool after cutting and in this way σ and τ were calculated. Using the present theory it is possible to predict h from the cutting conditions.

Consider the position of the resultant cutting force. This must have the same value whether it is calculated from the stresses in the shear zone or from the stresses along the tool-chip interface. By taking moments of the normal stress on AB (Fig. 5) about B it can be shown that the resultant cutting force cuts the tool-chip interface at a distance

$$x = \frac{2\ t \sin (\phi + \lambda - \alpha)}{\cos \lambda \sin \phi} \left\{ \frac{\frac{1}{3} p_A + \frac{1}{6} p_B}{p_A + p_B} \right\} \tag{24}$$

above the cutting edge. Following the experimental work of Zorev[11], and Usui and Takeyama[12], in which the stresses along the tool-chip interface were measured by cutting with a photoelastic tool, let us idealize the normal stress distribution along the interface to a triangular distribution; the maximum stress being at the cutting edge. For this stress distribution:

$$x = \frac{h}{3} \tag{25}$$

Therefore, equating equations (24) and (25) we obtain the expression:

$$h = \frac{t \sin (\phi + \lambda - \alpha)}{\cos \lambda \sin \phi} \left\{ \frac{2p_A + p_B}{p_A + p_B} \right\} \tag{26}$$

Equations (22), (23) and (26) have been used to calculate σ and τ for different rake angles using experimentally measured values of λ. Fig. 15 gives the results of these calculations. Perhaps the most interesting result is the approximately constant value of τ at a value of roughly half the shear flow stress k (also plotted on Fig. 15). This result is similar to that found experimentally in reference 10 and suggests an interesting possibility. Up to the present time all cutting theories have had to specify the angle of tool-chip friction λ as starting information. Unfortunately, it has not been found possible to measure λ other than by making cutting tests, and it appears that λ is not a fundamental property in the accepted sense but is dependent on such parameters as tool rake angle. If now we can assume that the shear stress τ along the interface is reasonably constant (or varies in some predictable way) then it might be possible to replace λ by τ as starting information. This possibly is now being looked into.

6. Discontinuous Chip formation

Even when cutting relatively ductile materials certain changes in the cutting conditions are known to give a transition from a continuous to a discontinuous or partially discontinuous chip. That is, the chip cracks in the region of B (Fig. 5) and the crack sometimes extends to the chip free surface. Such chip formation gives a rough surface finish and also tends to leave cracks in the surface which lower the fatigue life of the machined component. The changes in cutting conditions which are known from practice to give a discontinuous chip are: a decrease in cutting speed, an increase in depth of cut t and a decrease in positive rake angle. Let us now consider these changes in the light of the theory.

At present it is not possible to predict from a given state of stress, strain and strain rate whether or not a material will crack. It seems reasonable, however, to assume that the lower the compressive value of the hydrostatic stress at B (Fig. 5) the more likely is the chip to crack in this region. Values of p_B calculated from the theory are given in Figs. 16 and 17 and it can be seen that a decrease in cutting speed or rake angle and an increase in depth of cut all give a decrease in p_B. The theory therefore gives a qualitative explanation of why these changes tend to give a discontinuous chip. In order to make a quantitative analysis a suitable crack criterion is needed.

7. A work-hardening 'Machinability' index

Engineers have been trying for many years to find some property (or properties) of a material which can be measured relatively easily and which will indicate the materials machining characteristics, i.e. its machinability. Machinability is assessed in terms of tool life, properties of the produced surface (e.g. surface finish) and cutting forces. It is not surprising that with such diverse considerations attempts to find a satisfactory machinability index have failed.

Let us consider machinability in terms of shear angle. This is a reasonable first step as large values of shear angle are associated with relatively low cutting forces, continuous chip formation and good surface finish. It is also possible that tool life is related in some way to shear angle, large shear angles giving relatively small cutting forces and hence, possibly, a longer tool life.*

In calculating ϕ (see specimen calculation page 7) it is found that for given cutting conditions an increase in the value of $\frac{m}{k}$ (i.e. slope of plastic shear stress - shear strain curve divided by shear flow stress along AB (Fig. 5)) gives a decrease in ϕ. That is, the larger the value of $\frac{m}{k}$ the smaller is the value of ϕ.

Unfortunately, the values of $\frac{m}{k}$ for materials at high strain-rates are not known. It seems reasonable, however, to assume at this stage that a material which has a high value of $\frac{m}{k}$ as measured by say a compression test will have a comparatively high value of $\frac{m}{k}$ at high strain-rates.

Following this line of reasoning we can propose that materials which have high 'static' values of $\frac{m}{k}$ will in general machine with smaller values of ϕ than those with small values of $\frac{m}{k}$.

Figure 18 shows effective stress-effective strain curves obtained by Kobayashi and Thomsen [13] for different materials. To calculate $\frac{m}{k}$ (note: $k = \frac{\sigma_{eff}}{\sqrt{3}}$ and $\gamma = \sqrt{3}\,\epsilon_{eff}$) for these materials we will take the value of k corresponding to an effective strain of 0.5 i.e. a shear strain along AB of approximately unity which is of the same order as that met in cutting. The value of the slope m will be taken as the average slope above an effective strain of 0.2, it having been shown[14] that it is the slope at high strains rather than the initial slope which is important in cutting.

Values of $\frac{m}{k}$ for the materials shown in figure 18 are given in table 1. From this table we would expect the range of values of ϕ to be lowest for alpha brass and then in the order SAE 1112 Annealed, SAE 1112 as received, 6061-T6 Aℓ, and 2024-T4 Aℓ. Experimental values of ϕ for these materials (Fig. 19) confirm this trend.

---

* Metallurgical properties of the work and tool materials are of course of vital importance in considering tool life and these are not considered in this paper.

	MATERIAL	m/k
1	SAE 1112 steel (as received)	.14
2	2024-T4 aluminium alloy	.10
3	SAE 1112 steel (annealed)	.25
4	6061-T6 aluminium alloy	.11
5	Alpha brass	.42

TABLE 1

Figure 20 shows stress-strain curves for four conditions of SAE 4135 steel and table 2 gives the corresponding values of $\frac{m}{k}$. Experimental values

	MATERIAL	m/k
1	SEA 4135 (Rc - 35)	.06
2	SAE 4135 (Rc - 26)	.09
3	SAE 4135 (as received)	.21
4	SAE 4135 (annealed)	.21

TABLE 2

of ϕ (Figs. 21 and 22) for the four conditions of the material again show that the higher the value of $\frac{m}{k}$ the lower is the range of values of ϕ. Cutting tests now being made at Cranfield are giving similar results.

The actual value of k is important in determining the magnitudes of the cutting forces and stresses acting on the cutting tool. Even with large values of shear angle a high value of k will give large cutting forces and stresses. Therefore, in considering the machinability of a material account must be taken of both $\frac{m}{k}$ and k. Materials with large values of both these parameters can be expected to fall in 'the difficult to machine' range of materials.

8. Discussion

In the analysis, the variation of shear flow stress with strain and strain-rate has been taken into account in a fundamental manner, i.e. in the equilibrium equation. In this way, experimentally observed trends in metal cutting, for example the decrease in a shear angle and the tendency for the chip to become discontinuous with reduction in cutting speed, have been explained satisfactorily for the first time. In making the analysis a number of idealising assumptions were made. Let us now consider these in some detail.

It would be naive to imagine that for all materials and cutting conditions,

the length to width ratio (i.e. $\frac{t}{\Delta s_1 \sin\phi}$) of the shear zone remained constant. Also we know that the zone is not parallel sided, but varies in width (Figs. 1 and 2). Experiments using high speed cine and scribed grid techniques should be made to examine the size and shape of the shear zone over a wide range of conditions. Results from such experiments would show how the shear zone varied and also would help in understanding the fundamental mechanism which determines the size and shape of the shear zone. Information would also be obtained on the way in which the strain rate (a mean value was assumed in the analysis) varies in the shear zone and the mechanism by which the chip is 'born' curled. Detailed examination of the flow near the cutting edge will throw light on built-up edge formation, discontinuous chip formation and the way in which the properties of the newly machined surface (e.g. the residual stresses) are determined.

The values of the slope m and initial shear flow stress k which were used (Figs. 10 and 11) in the calculations were obtained by analysing cutting data. It is clear that independent methods for measuring these parameters are needed if the theory is to be used predictively, that is, without first making cutting tests.

The difficulty of describing the frictional condition along the tool-chip interface has already been mentioned. If, as is usual, it is represented by a mean angle of friction, then it is found that the only method of measuring the angle of friction is by cutting tests. An alternative approach, in which the friction along the interface is thought of in terms of the shear flow stress along the interface is now being considered. Preliminary results suggest that in this way the variations in friction which occur, for example, with rake angle can be far more easily understood.

The ratio $\frac{m}{k}$ (slope divided by shear flow stress) has been suggested as a possible machinability index. In future work on machinability it would be useful to measure $\frac{m}{k}$ to see if the correlation between $\frac{m}{k}$ and shear angle (Figs. 18, 19, 20, 21 and 22) has any wider significance e.g. is this parameter related to tool life.

In conclusion, it is hoped that the basically new approach to the machining problem presented in this paper will help suggest possible lines for future investigations.

References

1.	H. Ernst	Trans. Amer. Soc. Metals 'Symposium on Machining of Metals, I. Physics of Metal Cutting' (1938)
2.	M.E. Merchant	J. Appl. Phys. 16, 267 and 318 (1945)
3.	F.H. Lee and B.W. Shaffer	J. Appl. Mech. 18, 405 (1951)
4.	S. Kobayashi and E.G. Thomsen	Trans. A.S.M.E. paper 61-Prod-2 (1961)
5.	W.B. Palmer and P.L.B. Oxley	Proc. Inst. Mech. Engrs 173,24,623 (1959)
6.	D. Kececioglu	Trans. A.S.M.E. 80,158 (1958)
7.	K. Nakayama	J. Soc. Prcn. Mech., Japan 23,491 (1957)
8.	H. Enaharo	Private communication to the author
9.	P.L.B. Oxley	A.S.M.E. Paper No. 62-WA-139 (1963)
10.	J.H. Creveling., T.F. Jordan and E.G. Thomsen	Trans. A.S.M.E. 79,127. (1957)
11.	N.N. Zorev	Inst. Mech. Engrs. Conf. Technology of Engineering Manufacture 255 (1958)
12.	E. Usui and H. Takeyama	Trans. A.S.M.E. 82,303 (1960)
13.	S. Kobayashi and E.G. Thomsen	Trans. A.S.M.E. 81,251 (1959)
14.	P.L.B. Oxley., A.G. Humphreys and A. Larizadeh	Proc. Inst. Mech. Engrs. 175,18,881 (1961)
15.	P.L.B. Oxley	Leeds University, Ph.D. Thesis (1957)
16.	M.C. Shaw., N.H. Cook and I. Finnie	Trans. A.S.M.E. 75,273 (1953)
17.	E.G. Thomsen., J.T. Lapsley and R.C. Grassi	Trans. A.S.M.E. 75,591 (1953)
18.	S. Kobayashi., R.P. Herzog, D.M. Eggleston and E.G. Thomsen.	Trans. A.S.M.E. 82,333 (1960)

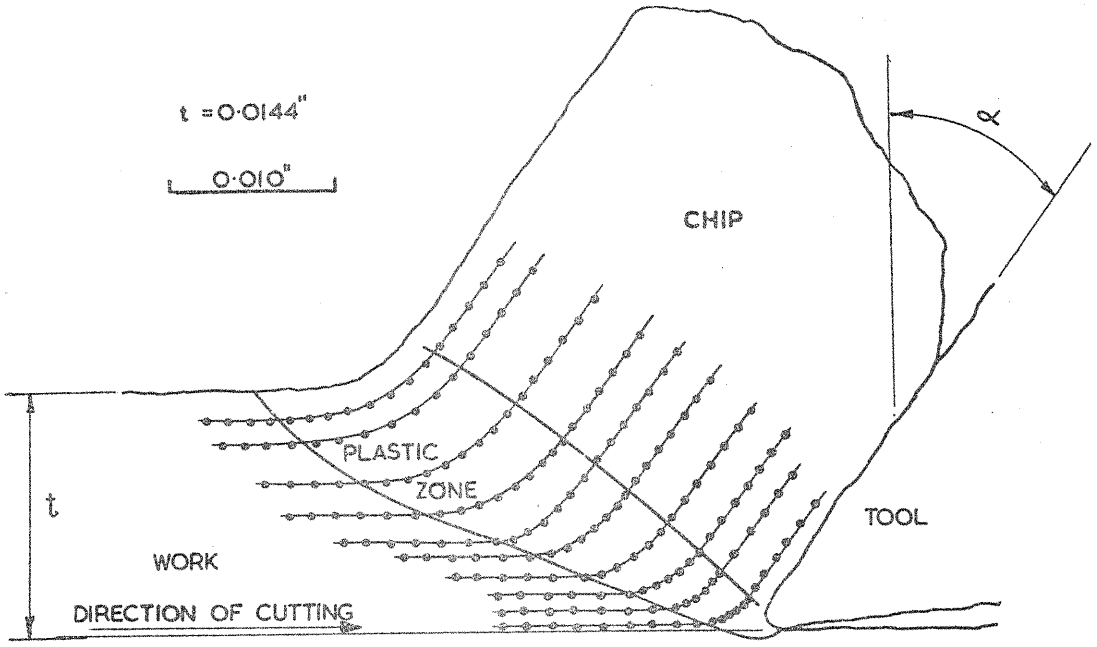

FIG. 1. PLASTIC ZONE (CUTTING SPEED $\frac{1}{2}$ in./min.)

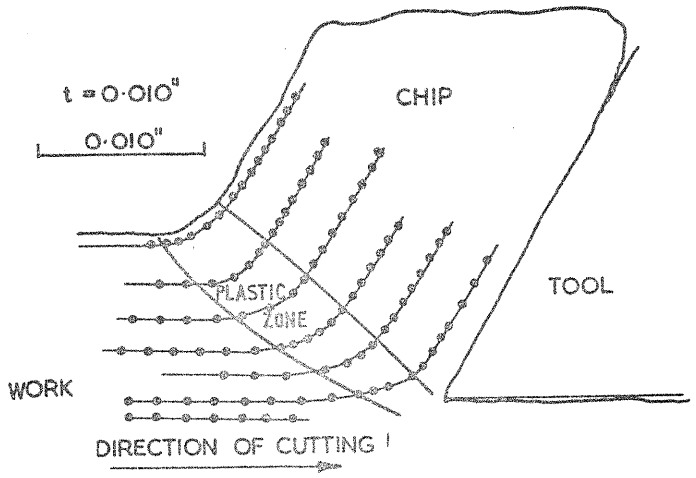

FIG. 2. PLASTIC ZONE (CUTTING SPEED 50ft/min.)

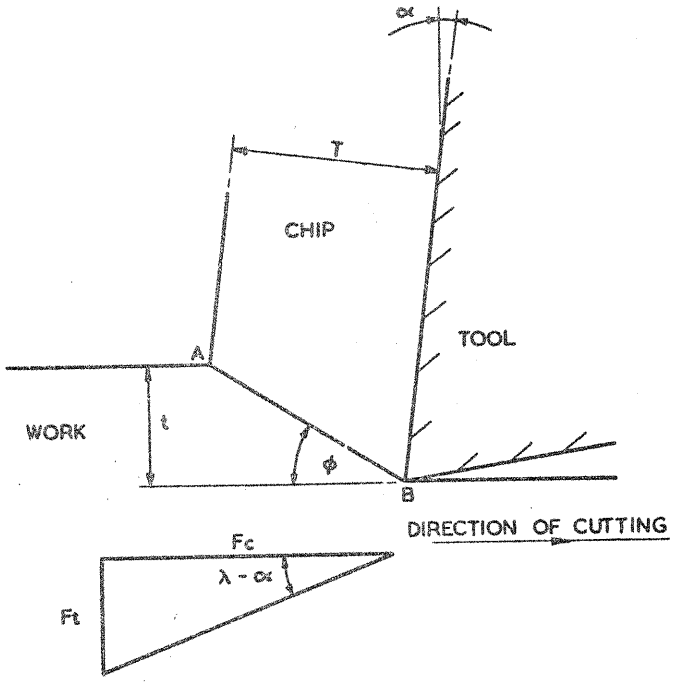

FIG. 3. SHEAR PLANE MODEL OF CHIP FORMATION

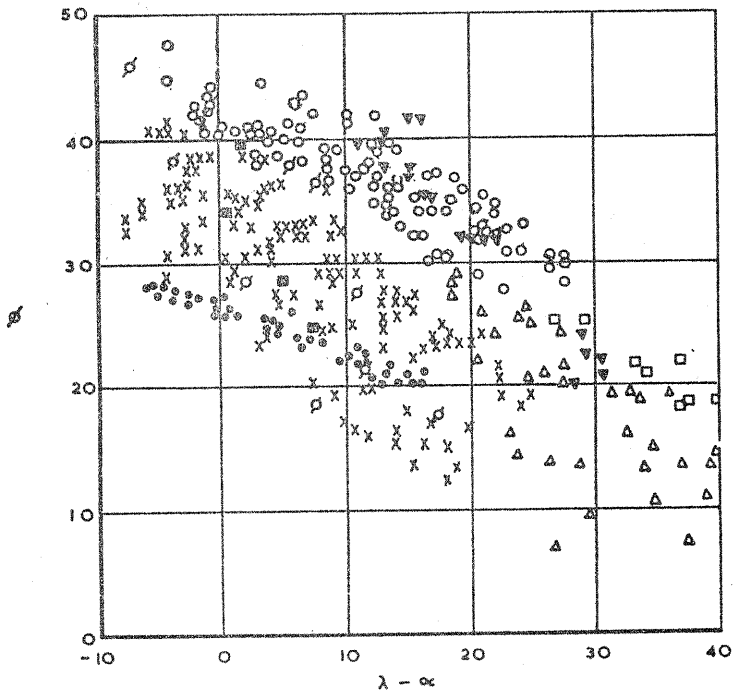

FIG. 4 Experimental values of shear angle

Experimental points:
Merchant [2]
Oxley [15]
Kececioglu [6]
Kobayashi and Thomsen [13] — Alpha brass, Aluminium, SAE 1112
Shaw, Cook and Finnie [16]
Thomsen, Lapsley and Grassi [17]

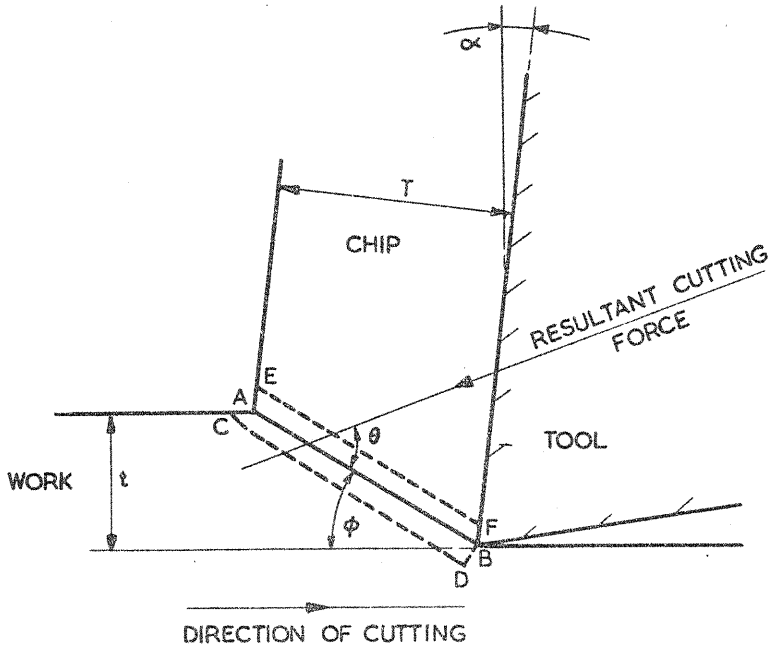

FIG. 5. SHEAR ZONE MODEL OF CHIP FORMATION

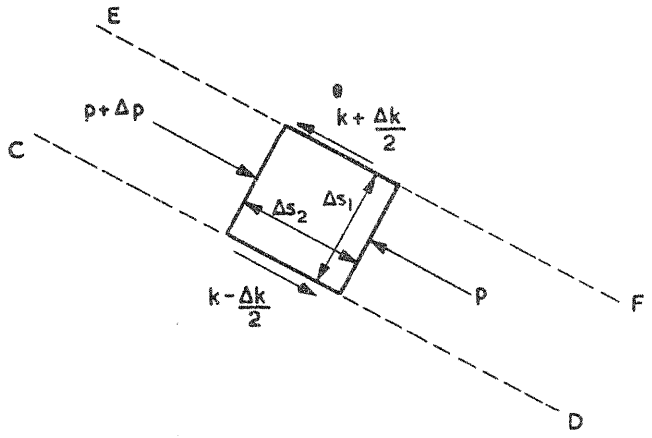

FIG. 6. SHEAR ZONE ELEMENT

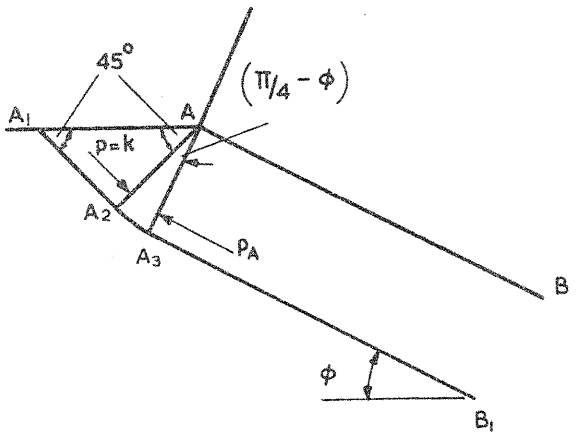

FIG. 7. SHEAR ZONE ELEMENT AT FREE SURFACE

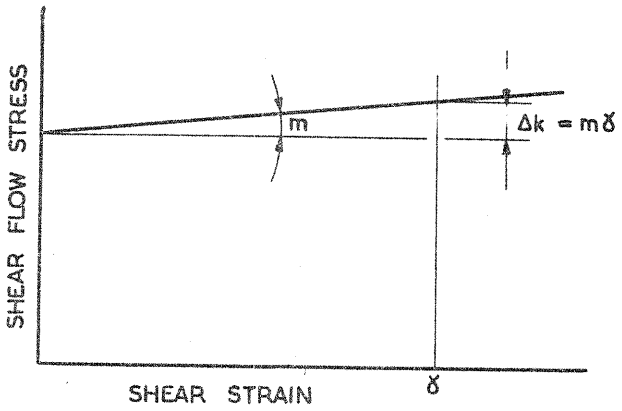

FIG. 8. IDEALIZED STRESS - STRAIN CURVE

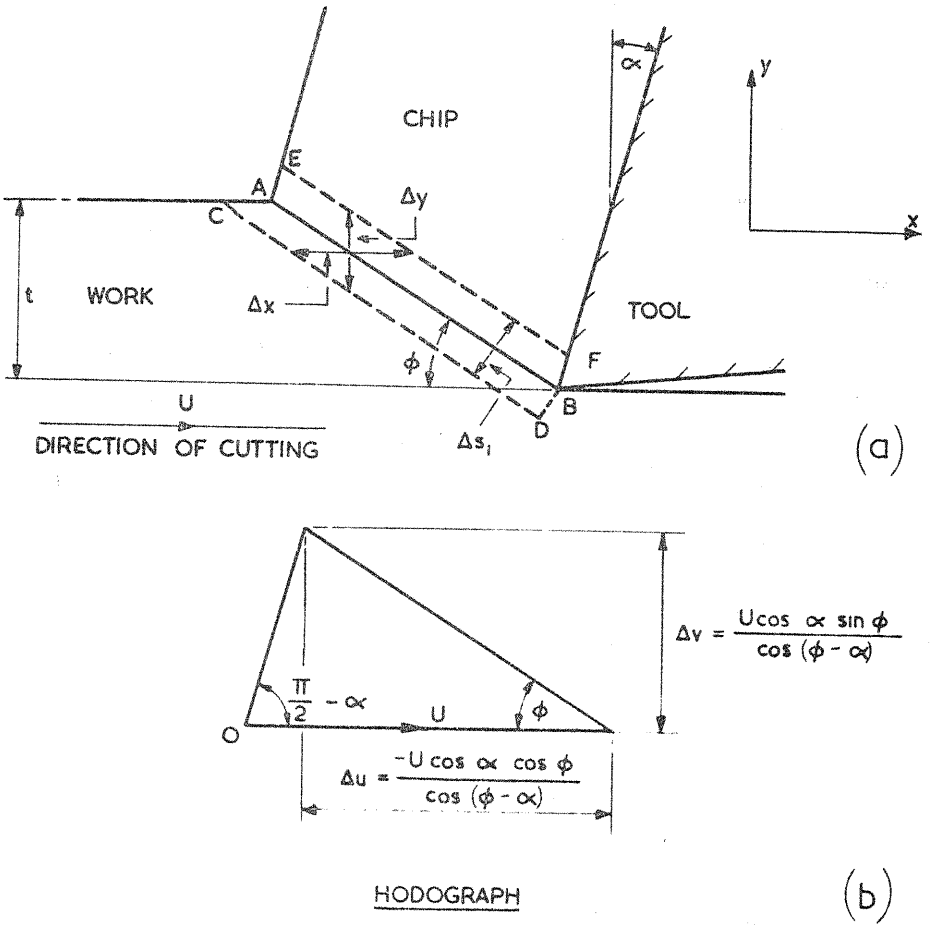

FIG. 9. SHEAR ZONE AND HODOGRAPH

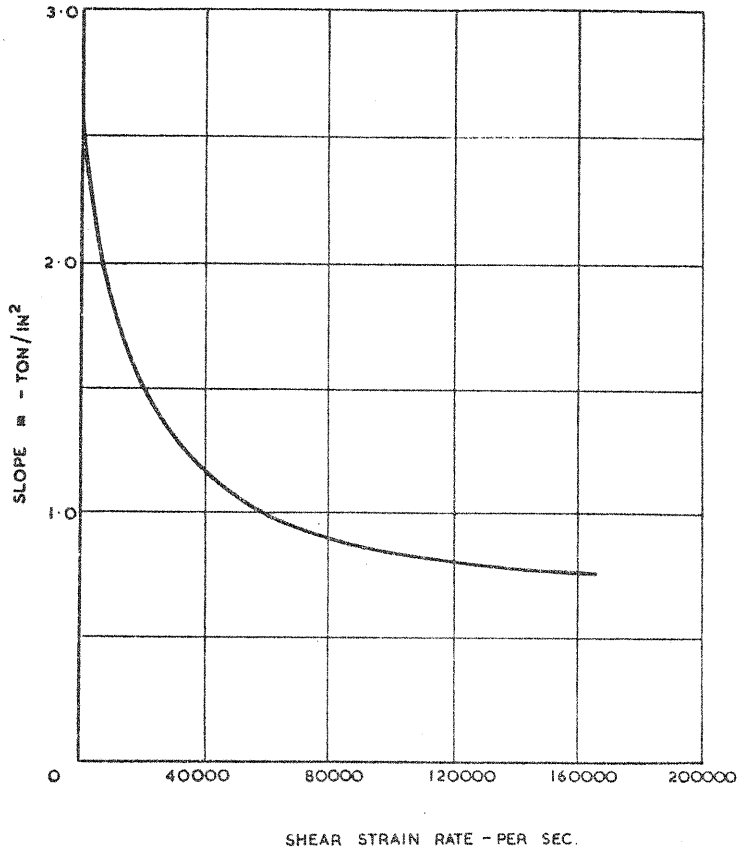

FIG.10 Slope m.

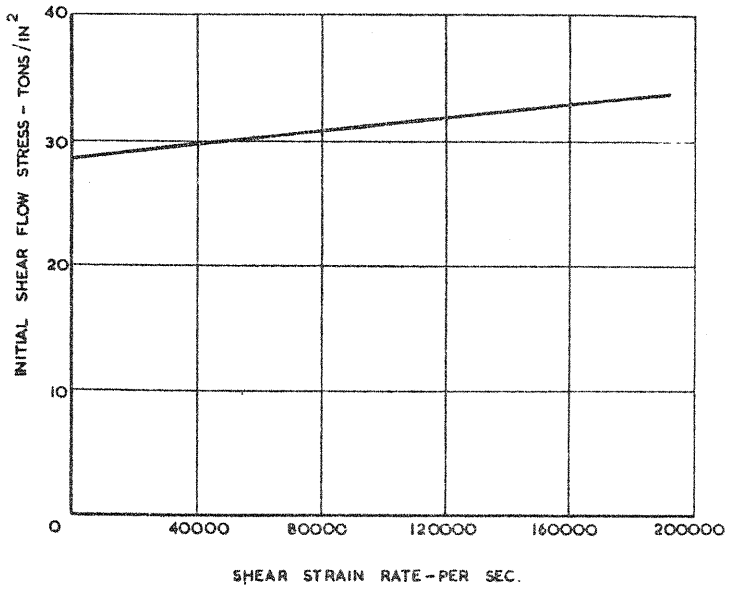

FIG.11 Initial shear flow stress.

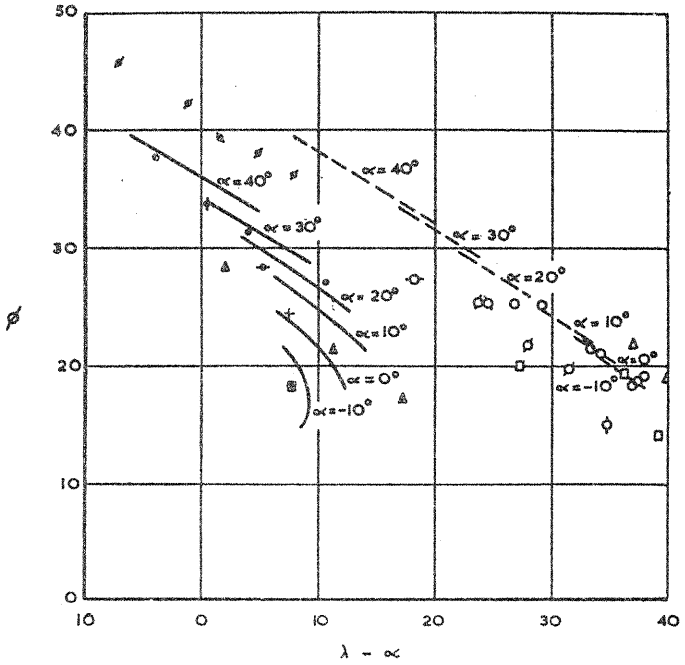

FIG. 12 Influence of cutting speed on shear angle.

Broken lines theoretical curves for 0·010 in. depth of cut, cutting speed 1000 ft/min, rake angles from −10° to 40°.
Unbroken lines theoretical curves for similar cutting conditions but 1 in./min cutting speed.
Experimental points:

Merchant [2]	$\alpha =$ 10°	○	400–1160 ft/min
	$\alpha =$ −10°	△	
Kececioglu [6]	$\alpha =$ −10°	□	
	$\alpha =$ 4°	○	
	$\alpha =$ 19·5°	⬠	746 ft/min
	$\alpha =$ 33°	⬡	
	$\alpha =$ 36·5°	⯃	
Shaw, Cook and Finnie [16]	$\alpha =$ 0°	▩	
	$\alpha =$ 16°	▲	
	$\alpha =$ 30°	●	1 in./min
	$\alpha =$ 40°	◪	
Oxley [15]	$\alpha =$ 25°	+	
	$\alpha =$ 30°	⊕	0·5 in./min
	$\alpha =$ 35°	◉	
	$\alpha =$ 40°	◍	

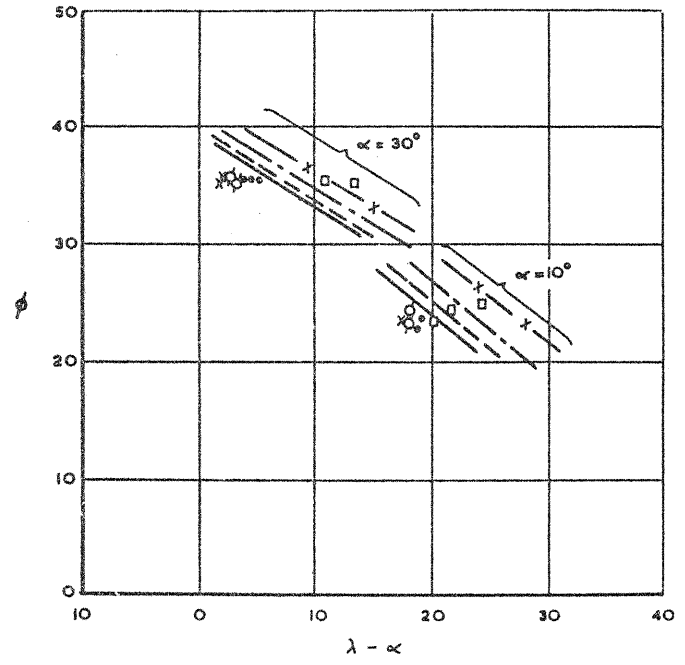

FIG. 13 Influence of depth of cut on shear angle.

Theoretical curves, cutting speed 100 ft/min
Rake angles 30° and 10°
Depth of cut 0·002 in. —— × —— × ——
0·004 in. — — — — — —
0·006 in. — — — — — —
0·008 in. ————————

Experimental points:
Kobayashi and Thomsen [13]
Cutting speed 90·8 ft/min
Rake angles 30° and 10°

0·00198 in.	□
0·00401 in.	●
0·00631 in.	⬠
0·00802 in.	×

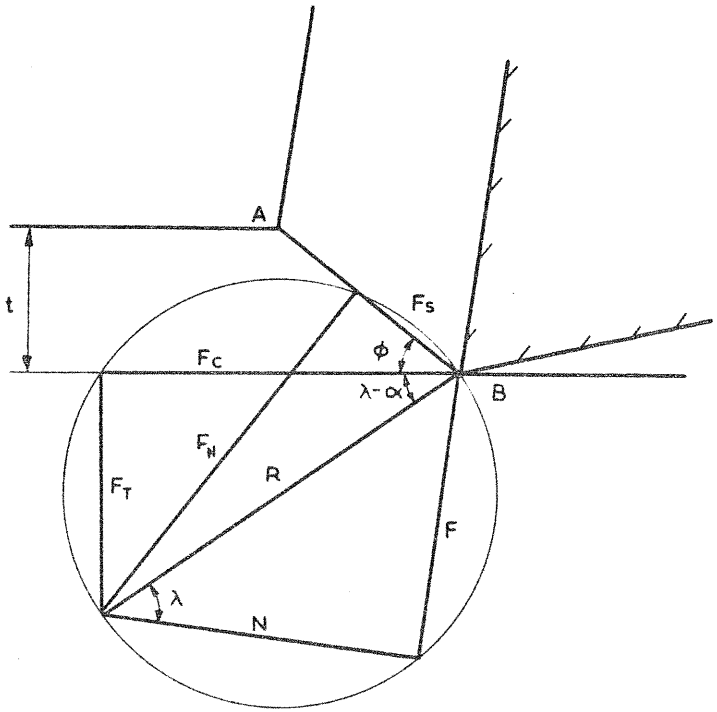

FORCES PER UNIT WIDTH ARE :-

$$F_s = \frac{tk}{\sin\phi} \qquad R = \frac{F_s}{\cos(\phi+\lambda-\alpha)} = \frac{tk}{\sin\phi\cos(\phi+\lambda-\alpha)}$$

$$F_c = R\cos(\lambda-\alpha) \qquad F = R\sin\lambda$$

$$F_T = R\sin(\lambda-\alpha) \qquad N = R\cos\lambda$$

FIG. 14. CUTTING FORCES

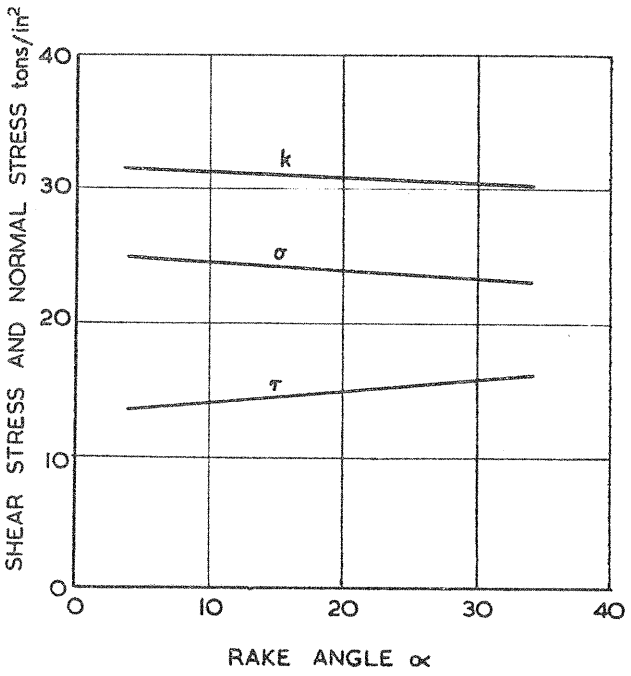

FIG. 15. TOOL-CHIP INTERFACE STRESSES

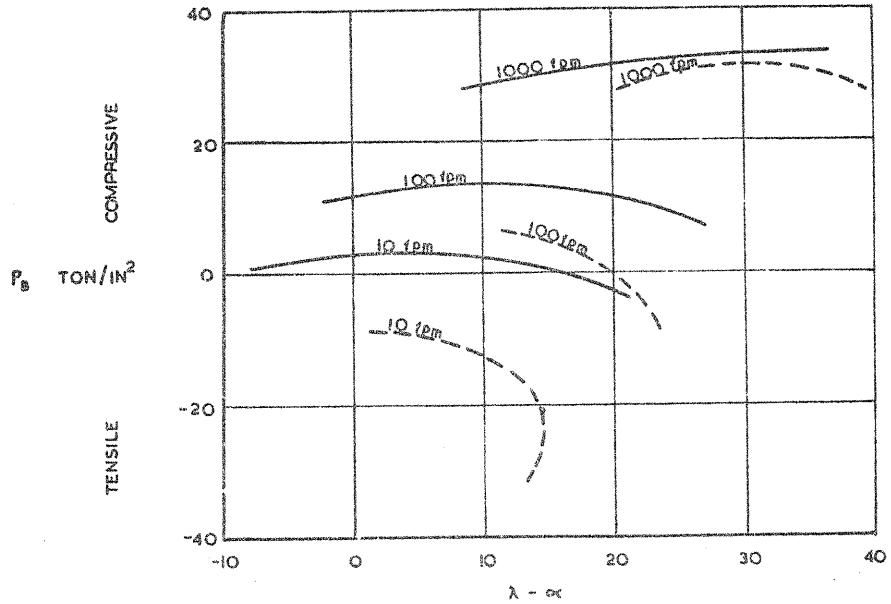

FIG. 16 Influence of speed on the hydrostatic stress p_B at the tool cutting edge.

Theoretical curves, cutting speed 10, 100 and 1000 ft/min, depth of cut 0·010 in.,
$a = 30°$ ————————
$a = 10°$ — — — — — —

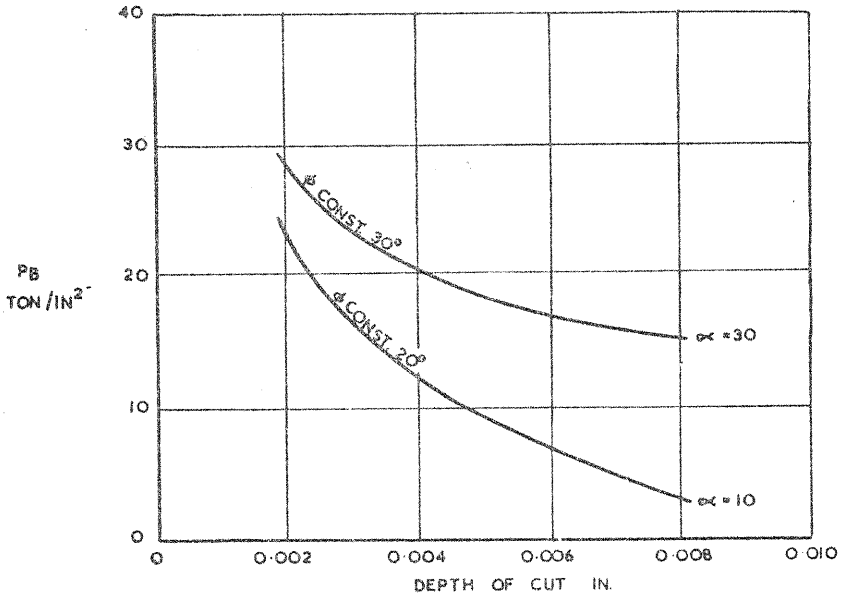

FIG. 17 Influence of depth of cut on the hydrostatic stress p_B at the tool cutting edge.

Theoretical curves (ϕ const.) for rake angles of 30° and 10°, cutting speed 100 ft/min.

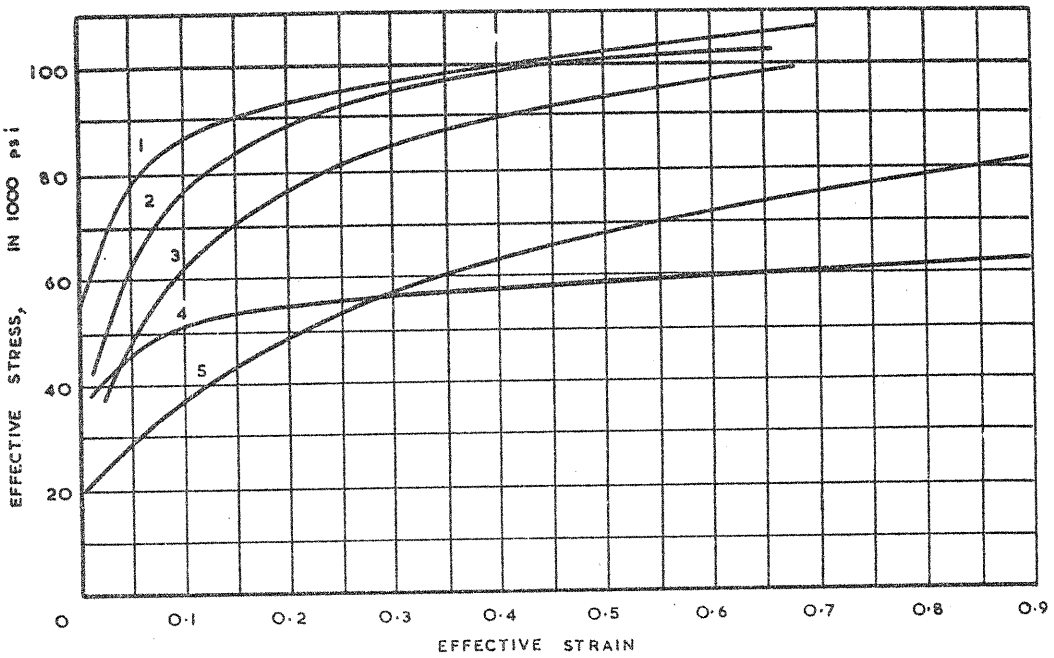

FIG. 18 Effective stress–strain curves (Kobayashi and Thomsen).[13]

1. SAE 1112 steel (as received)
2. 2024-T4 aluminium alloy
3. SAE 1112 steel (annealed)
4. 6061-T6 aluminium alloy
5. Alpha brass

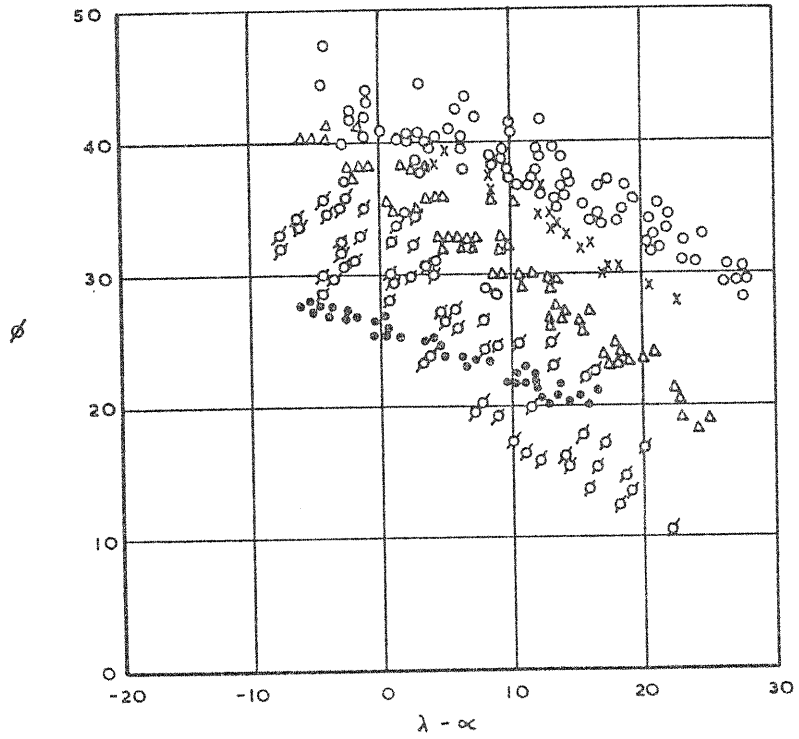

FIG. 19 Shear angle values for materials shown in Fig. 18 (Kobayashi and Thomsen).[13]

2024-T4 aluminium alloy ○
6061-T6 aluminium alloy ×
SAE 1112 steel (as received) △
SAE 1112 steel (annealed) ◇
Alpha brass ●

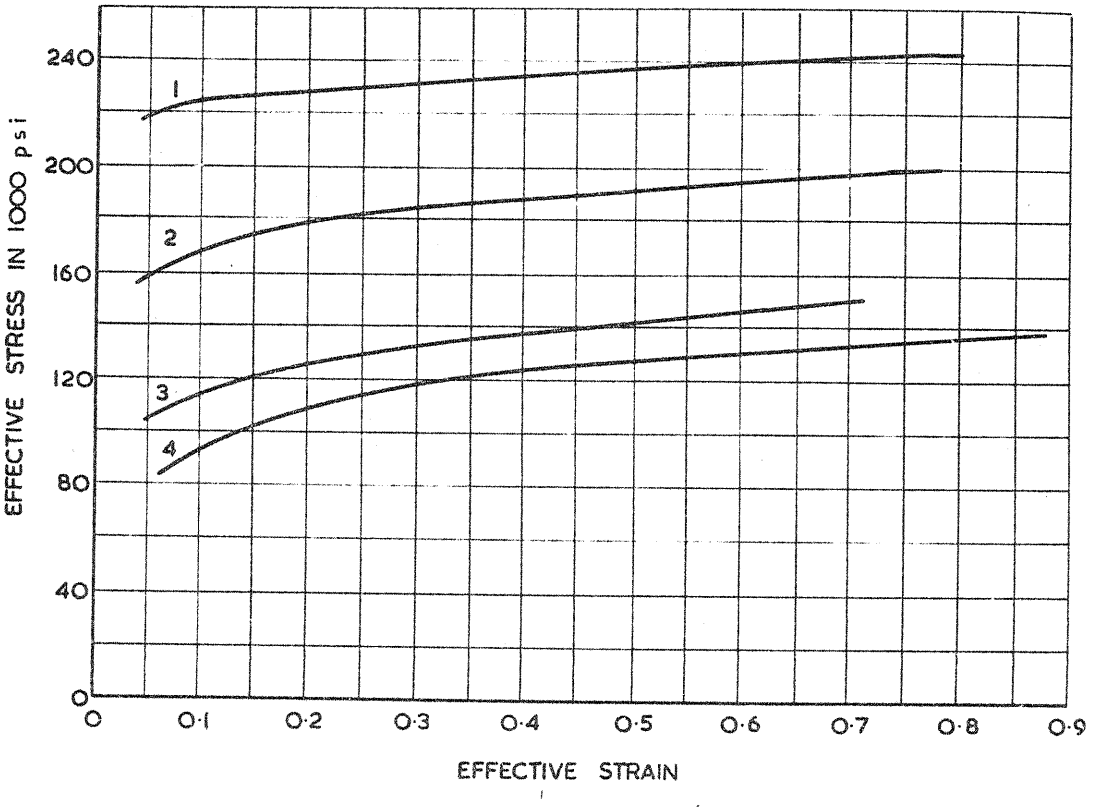

FIG. 20. EFFECTIVE STRESS-STRAIN CURVES (KOBAYASHI ET AL)[18]

1. SAE 4135 RC-35
2. SAE 4135 RC-26
3. SAE 4135 AS REC.
4. SAE 4135 Annealed

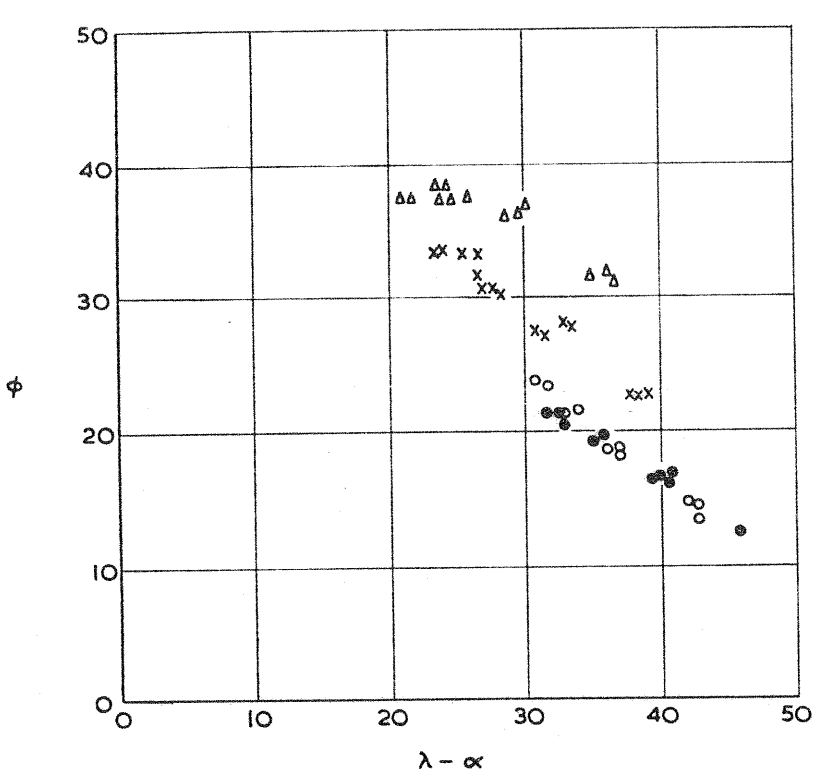

FIG. 21. SHEAR ANGLE VALUES FOR MATERIALS SHOWN IN FIG. 20.

$\alpha = 0^{\circ}$ U = 334 f.p.m.

SAE 4135 RC-35 Δ
SAE 4135 RC-26 x
SAE 4135 AS-REC o
SAE 4135 Annealed ●

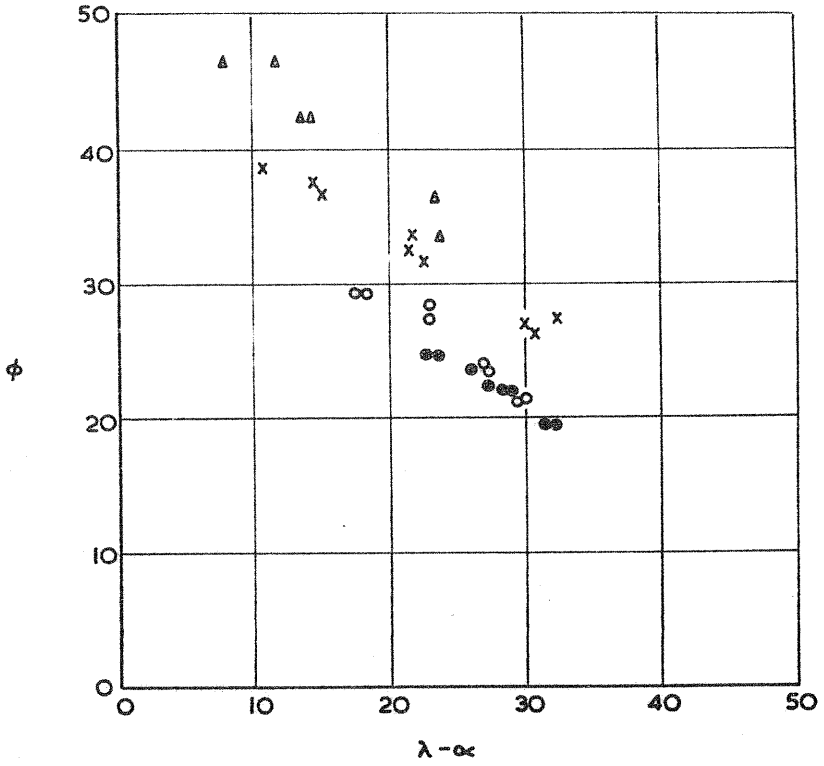

FIG. 22 SHEAR ANGLE VALUES FOR MATERIALS SHOWN IN FIG. 20.

$\alpha = 20^{\circ}$ U = 393 f.p.m.

SAE 4135 RC-35 Δ
SAE 4135 RC-26 x
SAE 4135 AS-REC o
SAE 4135 Annealed ●